Fig. 3. Solitary VCSEL characteristics obtained for $I = 45.0$mA and $T_{sub} = 25.0°$C. (a) near fiel profil in the transverse plane. Black corresponds to high optical power whereas white corresponds to low optical power. (b) is the corresponding optical spectrum.

2.3. Optically injected VCSEL

Finally, we examine the spectrum of the VCSEL submitted to optical injection with a polarization direction parallel to the one of the VCSEL. We set the VCSEL current at $I = 45.0$mA and we keep the substrate temperature constant at $T_{sub} = 25.0°$C. Injection locking requires high enough injected power as well as a negative and small enough frequency detuning [66]. For this purpose, we need an injection wavelength greater than 982.91nm. The measurement of the optical spectra is shown in Fig. 4. These spectra have been measured for two values of the injected power determined by the photodiode PD_1. When the injection beam power is $P_{inj} = 850 \mu$W, the VCSEL is frequency pulled towards the master laser frequency which is indicated by a short vertical arrow, as shown in Fig. 4(a). The near fiel emission profil changes, even if the fl wer-like mode has not disappeared from the emitting surface of the VCSEL. In this case, there is no injection locking of the VCSEL. However, for an injection power of $P_{inj} = 2.04$ mW, the VCSEL is locked to the master laser as shown in Fig. 4(b).
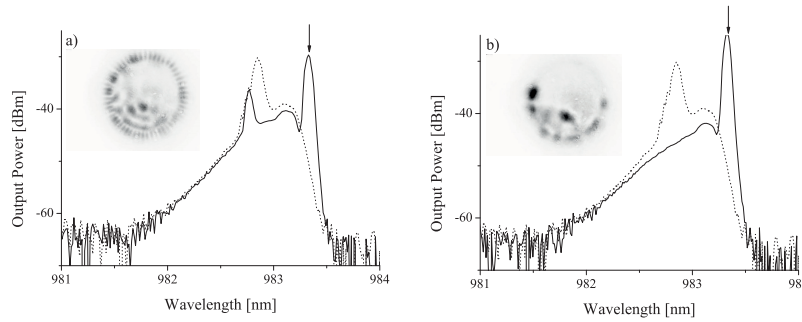

Fig. 4. Dashed lines: optical spectra of the free running VCSEL obtained for $I = 45.0$mA and $T_{sub} = 25.0°$C. Solid lines: optically injected VCSEL with $\lambda_{inj} = 983.24$nm (indicated by a vertical arrow) and injection power of (a) $P_{inj} = 850 \mu$W and (b) $P_{inj} = 2.04$ mW. The insets are near fiel images of the optically injected VCSEL.

3. Spontaneous formation of localized structures in an optically injected VCSEL

After the characterization of the VCSEL, we investigate the formation of two-dimensional localized structures in two different regimes. Our experimental setup possesses three control parameters, namely the injected power, frequency detuning, and the VCSEL current. This setup

may then undergo a bistable behavior when either varying the injected beam power or the VCSEL current. In addition, we study the formation of 2-dimensional LSs for different values of detuning and also for different beam waists. All experimental measurements have been performed when the VCSEL operated in an injection locked regime as in Fig. 4(b).

We firs investigated LSs bistable with the injection power for a f xed value of the detuning parameter $\theta = -174$ GHz and for a f xed value of the injection beam waist 100μm. The experimental results are summarized in the bistable curve in Fig. 5(a). The VCSEL output power as a function of the injected beam power, which is shown in this figure undergoes a bistable behavior between a single LS (i) and a two LSs (ii) states, as shown in Fig. 5(a). The experimental procedure to obtain LSs consists of increasing the injection power, and, just as the locking region is reached, a single LS appears. Then, as we further increase the optical injection power by tuning the variable optical density filte (VODF), we observe transition from a single LS state towards a two-LSs state. This behavior corresponds to a spontaneous switching on. To realise the switching off, we decrease the injection power. The two LSs persist until the system reaches the switching down point, over which the system relaxes to the single peak state. The density plot of both 1-LS and 2-LSs near fiel are recorded by using a CCD camera. Cross sections of the single and the two-LSs states near-fiel are shown in Figs. 5(b) and 5(c). A similar behavior of switching on and off has been observed while the detuning parameter was $\theta = -157$GHz and the beam waist 100μm. A fundamental characteristic of LSs is that it has
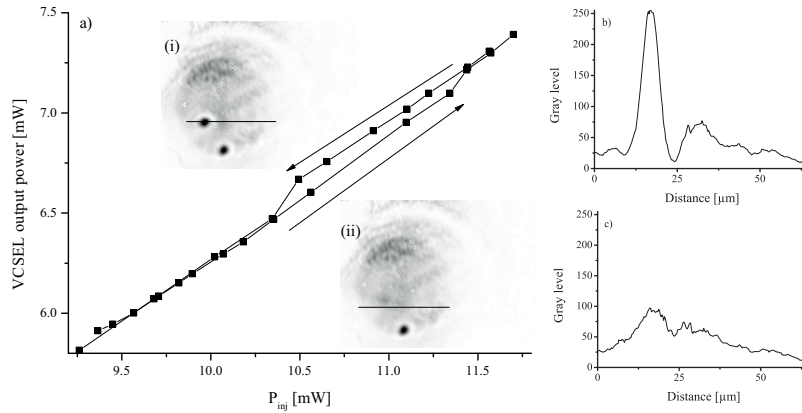

Fig. 5. Bistability between one and two-peaked LSs inside the near fiel of the VCSEL as a function of the optical injection power. (a): power emitted by the VCSEL as a function of the optical injection power for $\theta = -174$GHz and a beam waist of 100μm. The insets (i) and (ii) respectively represent near fiel profile on the higher and lower branch of the hysteresis. (b) and (c): one dimensional profile along the horizontal line drawn on the aforementioned insets.

an oscillatory tail, which decays exponentially with the distance to the center of the LS. This behavior has been shown experimentally with other optical systems [34, 35, 67]. We recover this fundamental property in VCSELs. An example of such a behavior is illustrated in Fig. 6.

In order to increase the optical power on the VCSEL, we decreased the beam waist to 50μm and the detuning to $\theta = -118$GHz. We could then reach a multipeak regime as shown in Fig. 7(a). In this case, three states can exist, with a bound state of two LSs (2P), this bound state accompagnied with a single peak localized structure (3P), or a four-peak LS (4P). Cross sections along the vertical lines in the insets Fig. 7 (2P), (3P) and (4P) coresspond to the aforementioned states. A bistable behavior has also been observed while the detuning was $\theta = -146$GHz.

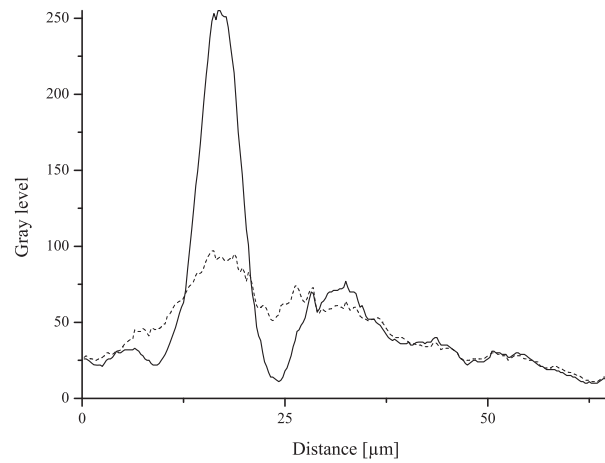Finally, a bistable behavior between two states is observed when varying the VCSEL current.

Fig. 6. Cross sections along the solid lines indicated in Fig. 5(a), (i) and (ii). The dashed line is the state (ii)(lower branch of the hysteresis), whereas the full line is the system with a LS (upper branch of the hysteresis).
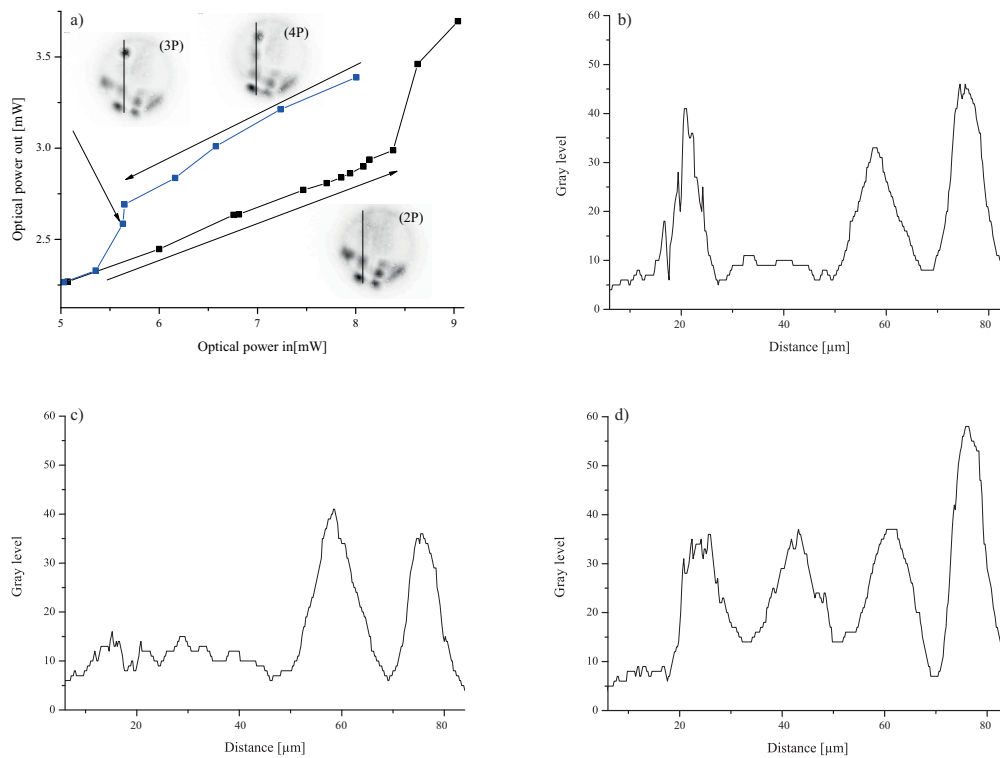

Fig. 7. Bistability between three states inside the near fiel of the VCSEL as a function of the optical injection power. (a): power emitted by the VCSEL as a function of the optical injection power for $\theta = -118$GHz and 50μm injection beam waist. The insets (2P) and (3P) and (4P) represent near fiel profile of the three possible states of the system. (b), (c) and (d): one dimensional profile along the vertical line drawn on the aforementioned insets.

We set the beam waist at 100μm and the optical injection power at 17mW. When varying the VCSEL current, we observe bistability of a LS. An example of such a behavior is illustrated in Fig. 8(a). Cross sections along the vertical lines in Figs. 8(b) and 8(c) correspond to the near fiel profile of the insets (i) and (ii), respectively.
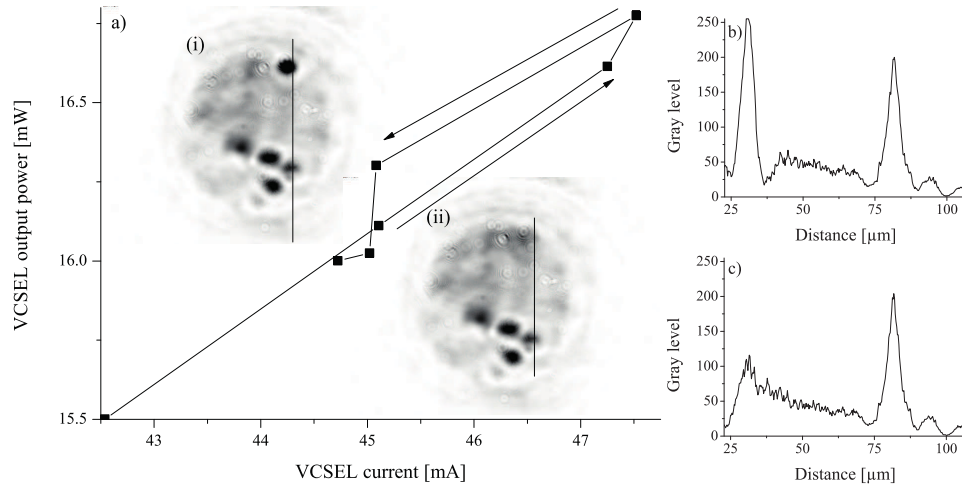

Fig. 8. Bistability between two states inside the near fiel of the VCSEL as a function of the VCSEL current. (a): power emitted by the VCSEL as a function of the VCSEL current for 100μm and 17mW optical injection beam waist and power, respectively. The bistable region of the curve has its detuning θ varying between -185GHz and -166 GHz due to the current induced thermal red shift. The insets (i) and (ii) represent near fiel profile of the two possible states of the system. (b) and (c): one dimensional profile along the vertical line drawn on the aforementioned insets.

4. Conclusions and perspectives

To conclude, we report experimental evidence of spontaneous formation of spatially localized structures in a 80μm diameter VCSEL submitted to optical injection. Different detunings between the frequencies of the injection beam and the VCSEL have been investigated, as well as different beam waists. This behavior occurs in two different bistability regimes by varying either the optical injection power or the VCSEL current.

In future work, we plan to investigate experimentally the role of delay feedback, and estabilsh a link with our predictions on a full rate equation model of broad area VCSELs [56, 57, 59] subject to simultaneous time-delayed feedback and optical injection. This study showed that the modulation instability region strongly depends on both the feedback strength and the feedback phase. Furthermore, the optical feedback induces traveling wave instabilities in the system, as well as spontaneous motion with a constant velocity of a single peak LS.

The analysis of local polarization dynamics [63] in the transverse plane of the resonator, the occurrence of polarization patterns and possibility the realization of LSs between two polarization modes can be of interest as well. Studies of vector solitons in polarization will be theoretically carried out using the spin-fli model of VCSELs, and implemented experimentally.

Acknowledgments